ARTICLE

ARFRP1 functions upstream of ARL1 and ARL5 to coordinate recruitment of distinct tethering factors to the trans-Golgi network

Morié Ishida and Juan S. Bonifacino

SNARE-mediated fusion of endosome-derived transport carriers with the trans-Golgi network (TGN) depends on the concerted action of two types of tethering factors: long coiled-coil tethers of the golgin family, and the heterotetrameric complex GARP. Whereas the golgins mediate long-distance capture of the carriers, GARP promotes assembly of the SNAREs. It remains to be determined, however, how the functions of these tethering factors are coordinated. Herein we report that the ARF-like (ARL) GTPase ARFRP1 functions upstream of two other ARL GTPases, ARL1 and ARL5, which in turn recruit golgins and GARP, respectively, to the TGN. We also show that this mechanism is essential for the delivery of retrograde cargos to the TGN. Our findings thus demonstrate that ARFRP1 is a master regulator of retrograde-carrier tethering to the TGN. The coordinated recruitment of distinct tethering factors by a bifurcated GTPase cascade may be paradigmatic of other vesicular fusion events within the cell.

Introduction

The TGN is a tubular-reticular organelle associated with the distal face of the Golgi stack that serves as a hub for multiple forward and retrograde pathways in the endomembrane system of eukaryotic cells (Griffiths and Simons, 1986; Guo et al., 2014). At the TGN, biosynthetic cargos coming from the Golgi stack are sorted to various post-Golgi compartments such as endosomes, lysosomes, secretory granules, different domains of the plasma membrane, and the extracellular space. The TGN also receives cargos by retrograde transport from endolysosomal compartments (Lu and Hong, 2014; Hierro et al., 2015). The delivery of retrograde cargos into the TGN occurs by SNARE-dependent fusion with tubular/vesicular carriers derived from endosomes. The SNAREs involved in this process include the Q-SNAREs syntaxin 6, syntaxin 16, and VTI1A, and an R-SNARE, VAMP4 or VAMP3, which assemble into a heterotetrameric trans-SNARE complex to enable merger of the carrier and TGN membranes (Mallard et al., 2002). In vivo, the specificity and efficiency of SNARE-dependent fusion events depend on two distinct classes of tethering factors known as homodimeric long coiled-coil proteins and multisubunit tethering complexes (MTCs; Yu and Hughson, 2010). At the mammalian TGN, four homodimeric long coiled-coil proteins named Golgin-245 (Yoshino et al., 2005), Golgin-97 (Lu et al., 2004), GCC185 (Reddy et al., 2006; Derby et al., 2007), and

GCC88 (Lieu et al., 2007; belonging to a family termed "golgins," reviewed by Cheung and Pfeffer, 2016; Fig. 1 A) and at least one MTC, the heterotetrameric Golgi-associated retrograde protein (GARP) complex (Siniossoglou and Pelham, 2002; Conibear et al., 2003; Liewen et al., 2005; Quenneville et al., 2006; Pérez-Victoria et al., 2008; Bonifacino and Hierro, 2011; Fig. 1 B), promote the delivery of retrograde cargos to the TGN. Each class of tethering factors plays a distinct role in the fusion event: while the golgins mediate long-distance capture of the carriers (Wong and Munro, 2014; Cheung et al., 2015), GARP coordinates the assembly of the trans-SNARE complex (Siniossoglou and Pelham, 2002; Conibear et al., 2003; Quenneville et al., 2006; Pérez-Victoria and Bonifacino, 2009). The physiological importance of mammalian GARP is underscored by the embryonic lethality of mice with null mutations in GARP subunit genes (Bennett and Dunn, 1958; Schmitt-John et al., 2005; Sugimoto et al., 2012; Karlsson et al., 2013), the motor neuron degeneration caused by a hypomorphic mutation in the VPS54 subunit of GARP in the wobbler mouse (Schmitt-John et al., 2005; Pérez-Victoria et al., 2010a), and the neurodevelopmental abnormalities in human patients with hypomorphic mutations in GARP subunit genes (Feinstein et al., 2014; Hady-Cohen et al., 2018; Gershlick et al., 2019; Uwineza et al., 2019).

Cell Biology and Neurobiology Branch, Eunice Kennedy Shriver National Institute of Child Health and Human Development, National Institutes of Health, Bethesda, MD.

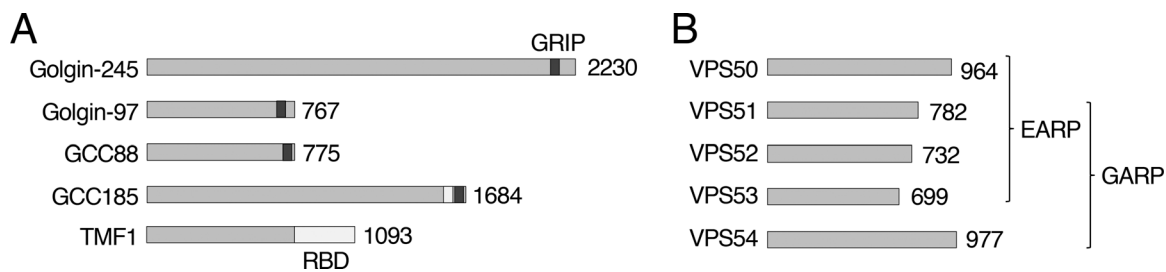Correspondence to Juan S. Bonifacino: juan.bonifacino@nih.gov.

Figure 1. **Characteristics of TGN tethering factors. (A)** Schematic representation of golgin coiled-coil tethers associated with the TGN (Golgin-245, Golgin-97, GCC88, and GCC185) and the late Golgi apparatus (TMF1). The location of a GRIP domain near the C terminus (black segment), a RAB6-binding region (RBD; light gray segment), and the total number of amino acids in each human protein are indicated. For additional details, see Cheung and Pfeffer (2016). **(B)** Schematic representation of GARP and EARP MTCs. GARP is composed of VPS51, VPS52, VPS53, and VPS54, whereas EARP is composed of VPS50, VPS51, VPS52, and VPS53. Amino acid numbers in the human proteins are indicated. For additional details, see Schindler et al. (2015).

In addition to SNAREs and tethering factors, a third type of proteins involved in the fusion of endosome-derived carriers with the TGN consists of small GTPases of the ARF-like (ARL; Donaldson and Jackson, 2011; Sztul et al., 2019) and RAB families (Pfeffer, 2017). ARL1 is required for the recruitment of Golgin-245 and Golgin-97 to the TGN through an interaction with an ~45-residue GRIP domain at or near the C terminus of these golgins (Lu and Hong, 2003; Panic et al., 2003a; Fig. 1 A). ARL1 appears less important for the recruitment of GCC185 and GCC88 to the TGN in mammals, despite the fact that these proteins also have a GRIP domain at their C termini (Derby et al., 2004; Burguete et al., 2008; Houghton et al., 2009; Torres et al., 2014). In the case of GCC185, an interaction of RAB6A with a region upstream of the GRIP domain (Fig. 1 A) promotes binding to ARL1 and thus contributes to association of GCC185 with the TGN (Burguete et al., 2008).

In contrast to the golgins, it is unclear how GARP is recruited to the TGN. In the yeast *Saccharomyces cerevisiae*, GARP was shown to interact with the GTP-bound forms of the Arl1p and Ypt6p orthologues of mammalian ARL1 and RAB6 (the latter of which occurs as RAB6A and RAB6B paralogs), respectively (Siniossoglou and Pelham, 2001; Panic et al., 2003b). However, deletion of yeast *ARL1* had no effect on the association of GARP with the late Golgi (equivalent of the mammalian TGN; Panic et al., 2003b), and deletion of yeast *YPT6* resulted in a more dispersed but still particulate distribution of GARP (Siniossoglou and Pelham, 2001). In higher eukaryotes, including *Drosophila melanogaster* and human cells, recruitment of GARP to the TGN was shown to depend on another member of the ARL family, ARL5 (Rosa-Ferreira et al., 2015). In humans, there are two ARL5 paralogs, ARL5A and ARL5B, both of which localize to the TGN (Houghton et al., 2012). siRNA-mediated knockdown (KD) of ARL5B, but not ARL5A, reduced retrograde transport from endosomes to the TGN (Houghton et al., 2012) as well as association of GARP with the TGN (Rosa-Ferreira et al., 2015). The specific requirement of ARL5B is probably due to its greater abundance relative to ARL5A in the HeLa cells that were used in those experiments (Rosa-Ferreira et al., 2015). Nevertheless, the dissociation of GARP from the TGN upon KD of ARL5B, alone or in combination with ARL5A, was incomplete, with 30–45% of the KD cells still retaining GARP staining at the TGN (Rosa-Ferreira et al., 2015).

The uncertainty about the factors that regulate the recruitment of mammalian GARP to the TGN prompted us to test the involvement of several Golgi-localized ARL and RAB GTPases by knocking out their genes in human HeLa cells and examining the localization of GARP by immunofluorescence microscopy. The use of knock-out (KO) cells avoided the incomplete depletion and off-target effects that are typical of siRNA-mediated KD. Using this approach, we found that double KO of ARL5A and ARL5B (hereafter referred to as ARL5 KO), but not ARL1 or double KO of RAB6A and RAB6B (referred to as RAB6 KO), abrogated the association of GARP with the TGN. Surprisingly, we observed that KO of another ARL-family member, ARFRP1, also abolished the recruitment of GARP to the TGN. Further experiments showed that ARFRP1 functions upstream of both ARL1 and ARL5 to promote the recruitment of three TGN golgins (Golgin-245, Golgin-97, and GCC88) and GARP, respectively, to the TGN. Our studies thus revealed that ARFRP1 functions as a master regulator of retrograde-carrier tethering by enabling the coordinated recruitment of two types of tethering factors to the TGN.

Results

ARL5 and ARFRP1 are required for GARP localization to the TGN

This project was initiated to identify small GTPases that regulate the recruitment of GARP to the TGN, by taking advantage of the ability to KO individual genes in HeLa cells using CRISPR/Cas9 technology. The mammalian GARP complex comprises four subunits named VPS51 (originally known as ANG2), VPS52, VPS53, and VPS54 (Liewen et al., 2005; Pérez-Victoria et al., 2008, 2010b; Fig. 1 B). A related complex named "endosome-associated recycling protein" (EARP) shares the VPS51, VPS52, and VPS53 subunits with GARP, but has an alternative subunit named VPS50 (also known as syndetin or VPS54L) in place of VPS54 (Gillingham et al., 2014; Schindler et al., 2015; Fig. 1 B). Unlike GARP, EARP is largely associated with an endosomal compartment and was not studied here (Gillingham et al., 2014; Schindler et al., 2015; Gershlick et al., 2019). Our attempts to detect endogenous GARP by immunofluorescence microscopy and immunoblotting using several commercially available antibodies to the GARP-specific VPS54 subunit were unsuccessful,

probably due to the low abundance of this protein in HeLa cells (~700 molecules per cell; Kulak et al., 2014). To overcome this limitation, we transfected HeLa cells with a plasmid encoding human VPS54 tagged at its C terminus with 13 copies of the Myc epitope (VPS54-13Myc). As previously reported (Schindler et al., 2015), this construct localized to a juxtanuclear structure characteristic of the TGN (Fig. S1 A, WT). This localization was abrogated by KO of VPS51, VPS52, or VPS53, but not VPS50, indicating that it reflected the distribution of the whole GARP complex (Fig. S1, A–C).

Next, we examined the effect of knocking out several TGN-localized small GTPases on the association of VPS54-13Myc with the TGN. We observed that KO of ARL1, ARL5 (i.e., both ARL5A and ARL5B paralogs), RAB6 (i.e., both RAB6A and RAB6B paralogs), or another member of the ARL family, ARFRP1 (Schürmann et al., 1995), completely abolished the expression of the corresponding proteins, as demonstrated by immunoblotting (Fig. 2 A and Fig. S2, A and B). KO of ARL1 or RAB6 had little or no effect on the localization of VPS54-13Myc to the TGN, but KO of ARL5 resulted in displacement of VPS54-13Myc to the cytosol (Fig. 2, B and C). This latter result was even more dramatic than that obtained by siRNA-mediated KD of ARL5 (Rosa-Ferreira et al., 2015), as it was observed in 100% of the cells. Surprisingly, KO of ARFRP1 also prevented association of VPS54-13Myc with the TGN (Fig. 2, B and C). From these experiments we concluded that ARL5 and ARFRP1 are both required for association of GARP with the TGN.

ARFRP1 functions upstream of ARL5 in GARP recruitment to the TGN

To investigate the functional relationship of ARL5 and ARFRP1 in the recruitment of GARP to the TGN, we performed a series of reciprocal rescue experiments. Expression of WT ARL5B-GFP in ARL5-KO cells restored the localization of VPS54-13Myc to the TGN (Fig. 3, A and B). Likewise, expression of WT ARFRP1-GFP in ARFRP1-KO cells rescued (albeit partially) the association of VPS54-13Myc with the TGN (Fig. 3, C and D). These experiments ruled out that the effects of the KOs on VPS54-13Myc localization were due to off-target effects. Like other small GTPases, ARL5 and ARFRP1 cycle between GTP-bound, active and GDP-bound, inactive forms (Donaldson and Jackson, 2011; Sztul et al., 2019). Rescue of VPS54-13Myc association with the TGN was also observed upon expression of constitutively active (Q70L) but not inactive (T30N) ARL5B-GFP in ARL5-KO cells (Fig. 3, A and B). Similarly, TGN localization of VPS54-13Myc was rescued by expression of constitutively active (Q79L) but not inactive (T31N) ARFRP1-GFP in ARFRP1-KO cells (Fig. 3, C and D). These results indicated that association of VPS54-13Myc with the TGN depends on the GTP-bound, active forms of ARL5 and ARFRP1. Importantly, whereas expression of WT or Q79L ARFRP1-GFP in ARL5-KO cells did not rescue the association of VPS54-13Myc with the TGN (Fig. 3, A and B), expression of WT or Q70L ARL5B-GFP in ARFRP1-KO cells partially rescued VPS54-13Myc association (Fig. 3, C and D). The ability of WT ARL5B-GFP to associate with the TGN and rescue VPS54-Myc localization in ARFRP1-KO cells (Fig. 3, C and D) suggests that a substantial fraction of this protein exists in the GTP-bound, active form

under the overexpression conditions of these experiments. Taken together, these results are consistent with ARFRP1 acting upstream of ARL5 to recruit GARP to the TGN.

We next wished to address whether endogenous ARL5 (as opposed to overexpressed WT ARL5B-GFP; Fig. 3 C) required ARFRP1 for association with the TGN. However, the antibodies to ARL5 that we tested worked for immunoblotting but not for immunofluorescence microscopy. Therefore, we fractionated cells into cytosol and membranes and immunoblotted for ARL5, ARL1, and RAB6. We observed that KO of ARFRP1 decreased the association of ARL5 and ARL1, but not RAB6, with membranes (Fig. 3, E and F). Rescue of these cells by expression of ARFRP1 restored normal levels of ARL5 and ARL1 membrane association. These analyses thus demonstrated that ARFRP1 is required for association of both ARL5 and ARL1 with membranes.

Impaired retrograde transport in ARL5-KO and ARFRP1-KO cells

GARP is required for delivery of retrograde cargos such as the TGN resident protein TGN46 and the Shiga toxin B subunit (STxB) from endosomes to the TGN (Pérez-Victoria et al., 2008, 2010a,b; Pérez-Victoria and Bonifacino, 2009). To determine if ARL5 and ARFRP1 are similarly required, we examined the distribution of TGN46 and the internalization of Cy3-conjugated STxB (Cy3-STxB) in ARL5-KO and ARFRP1-KO cells (Fig. 4). Indeed, we observed that KO of ARL5 or ARFRP1 caused dispersal of TGN46 from the TGN similar to that caused by VPS54 KO (Fig. 4 A), indicative of a defect in retrograde transport. As expected, TGN46 dispersal was prevented by expression of the corresponding GFP-tagged GTPase or VPS54 (Fig. 4 B). Interestingly, immunoblot analysis showed an increase in TGN46 species with faster electrophoretic mobility in cells with KO of ARL5, ARFRP1, or GARP subunits, but not VPS50 (Fig. 4 C). These differences were likely due to decreased carbohydrate modifications in the KO cells, as previously observed in cells from a patient with mutations in VPS51 (Gershlick et al., 2019). KO of ARL5, ARFRP1, or VPS54 also impaired the delivery of internalized Cy3-STxB (Johannes and Goud, 1998) to the Golgi complex (Fig. 4, D and E). These experiments thus demonstrated that ARL5, ARFRP1, and GARP are similarly required for retrograde transport to the TGN, consistent with the role of these small GTPases in the regulation of GARP.

ARFRP1 and ARL1, but not ARL5 or RAB6, are required for recruitment of Golgin-245, Golgin-97, and GCC88 to the TGN

Next, we investigated the possibility that the recruitment of GARP to the TGN is co-regulated with that of the TGN golgins. Previous studies showed that mammalian ARFRP1 and the orthologous yeast Arl3p promote recruitment of mammalian ARL1 (Shin et al., 2005; Zahn et al., 2006) and yeast Arl1p (Panic et al., 2003b; Setty et al., 2003), respectively, to the TGN. Thus, indirectly, ARFRP1/Arl3p contributes through ARL1/Arl1p to the recruitment of the GRIP domain–containing proteins Golgin-245 and Golgin-97 in mammals (Shin et al., 2005; Zahn et al., 2006) and Imh1p in yeast (Panic et al., 2003b; Setty et al., 2003). To develop a more global understanding of the small GTPase requirements for the recruitment of tethering factors to the TGN,
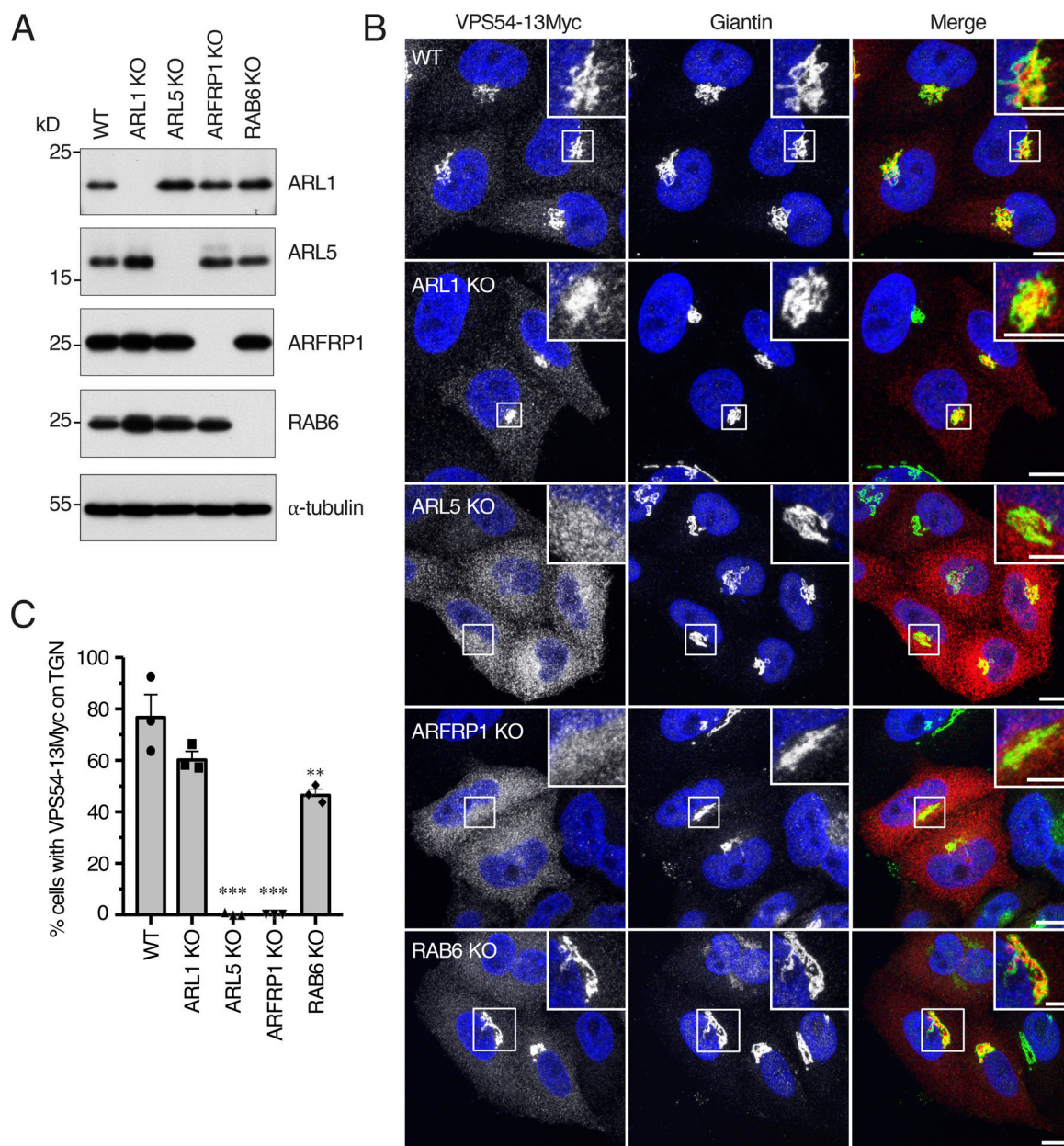
Figure 2. **Both ARL5 and ARFRP1 are required for localization of GARP to the TGN. (A)** KO of TGN-localized small GTPases in HeLa cells confirmed by immunoblot analysis with antibodies to the proteins indicated on the right. In this figure and subsequent figures, ARL5 KO represents KO of both ARL5A and ARL5B, and RAB6 KO represents KO of both RAB6A and RAB6B. α-Tubulin was used as a loading control. The positions of molecular mass markers are indicated on the left. **(B)** Immunofluorescence microscopy of WT and KO HeLa cells transfected with a plasmid encoding VPS54-13Myc and stained for the Myc epitope (red), giantin (green), and nuclei (DAPI; blue). Scale bars: 10 µm. Insets are magnified views of the boxed areas. Inset scale bars: 5 µm. **(C)** Quantification of the percentage of cells exhibiting VPS54-13Myc staining at the TGN. Values are the mean ± SEM from three independent experiments. More than 100 cells per sample were counted in each experiment. The statistical significance of the differences relative to WT cells was determined using Dunnett's test. **, $P < 0.01$; ***, $P < 0.001$.

we examined the effect of knocking out ARL1, ARL5, ARFRP1, or RAB6 on the association of Golgin-245, Golgin-97, GCC185, and GCC88 (Fig. 1 A) with the TGN. We observed that KO of ARL1 or ARFRP1 abrogated the association of Golgin-245 and GCC88, and, partially, Golgin-97, with the TGN (Fig. 5 A). In contrast, these KOs had little or no effect on the recruitment of the TGN golgin GCC185 and the Golgi-stack golgin TMF1 (used here as a control; Fig. 1 A and Fig. 5 A). Interestingly, and in line with these

observations, immunoblot analysis showed that KO of ARL1 or ARFRP1 reduced the levels of Golgin-245, Golgin-97, and GCC88, but not GCC185 (Fig. 5 B), indicating that association with the TGN is required for stability of these golgins. In contrast, KO of ARL5 or RAB6 had no effect on the TGN association (Fig. 5 A) or levels of any of these golgins (Fig. 5 B). RAB6 KO abolished the association of GCC185 with the TGN and of TMF1 with the Golgi stack (Fridmann-Sirkis et al., 2004; Fig. 5 A). The association of
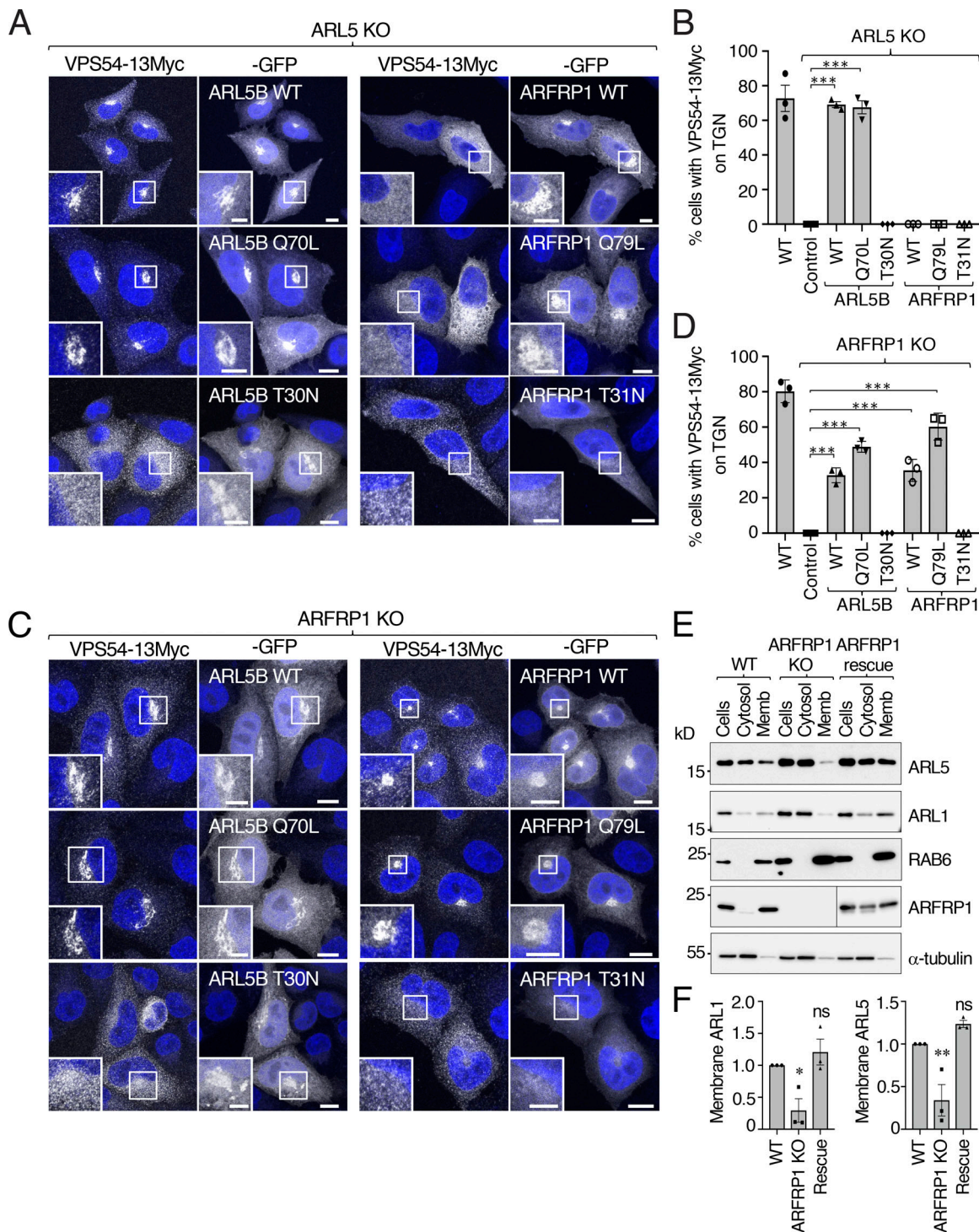
Figure 3. **ARFRP1 functions upstream of ARL5 for the recruitment of GARP to the TGN. (A)** GFP-tagged ARL5B (WT, Q70L, or T30N) or ARFRP1 (WT, Q79L, or T31N) were co-expressed with VPS54-13Myc in ARL5-KO cells. Cells were stained with DAPI (blue) and examined for GFP distribution by confocal microscopy. Scale bars: 10 µm. Insets are magnified views of the boxed areas. Inset scale bars: 5 µm. **(B)** The percentage of cells with VPS54-13Myc staining at the TGN was quantified as described in Fig. 2 C. Values are the mean ± SEM from three independent experiments. More than 100 cells per sample were counted in each experiment. ***, P < 0.001, in comparison to ARL5 KO cells only expressing VPS54-13Myc (control) using Dunnett's test. **(C)** GFP-tagged ARL5B (WT, Q70L, or T30N) or ARFRP1 (WT, Q79L, or T31N) were co-expressed with VPS54-13Myc in ARFRP1-KO cells. Cells were analyzed as in A. **(D)** Quantification of cells having VPS54-13Myc staining at the TGN as described in Fig. 2 C. Values are the mean ± SEM from three independent experiments. More than 100 cells per sample were counted in each experiment. ***, P < 0.001, in comparison to ARFRP1 KO cells only expressing VPS54-13Myc (control) using Dunnett's test. **(E)** Subcellular fractionation of WT, ARFRP1-KO, and ARFRP1-KO-rescue HeLa cells. Whole cells and cytosolic and membrane (Memb) fractions obtained as described in Materials and methods were analyzed by SDS-PAGE and immunoblotting for the proteins indicated on the right. The positions of molecular mass markers are indicated on the left. **(F)** Quantification of the ratio of membrane to the sum of membrane and cytosolic ARL1 and ARL5 protein from experiments such as that described in E. Ratios for ARFRP1-KO cells and ARFRP1-KO cells rescued with tag-less ARFRP1 were normalized to WT cells. Values are the mean ±

Ishida and Bonifacino
ARFRP1 coordinates tethering at the TGN

SEM from three independent experiments. The statistical significance of the differences relative to WT cells was determined using Dunnett's test. *, P < 0.05; **, P < 0.01.

GCC185 and TMF1 with the Golgi complex could be rescued by expression of GFP-Rab6A (mouse orthologue) in RAB6-KO cells (Fig. 5 C). These experiments therefore indicated that ARFRP1 and ARL1 regulate the recruitment of Golgin-245, Golgin-97, and GCC88, whereas RAB6 regulates the recruitment of GCC185, to the TGN.

ARFRP1 functions upstream of ARL1 in the recruitment of GCC88 to the TGN

Our finding that GCC88 requires ARFRP1 and ARL1 for recruitment to the TGN is at odds with the previous observation that GCC88 does not bind ARL1 in vivo (Derby et al., 2004). This discrepancy prompted us to analyze in further detail the functional interaction of GCC88 with ARFRP1 and ARL1. We observed that the association of GCC88 with the TGN in ARL1-KO cells could be rescued by expression of WT ARL1-GFP or active ARL1-GFP Q71L but not inactive ARL1-GFP T31N (Fig. 6, A and B). In contrast, ARFRP1-GFP failed to rescue GCC88 association with the TGN in ARL1-KO cells, irrespective of its activation state (Fig. 6, A and B). GCC88 localization to the TGN in ARFRP1-KO cells could also be restored upon expression of WT ARFRP1-GFP and active ARFRP1-GFP Q79L, but not inactive ARFRP1-GFP T31N (Fig. 6, C and D). In this case, however, expression of active ARL1-GFP Q71L, but not the other forms of ARL1-GFP, in ARFRP1-KO cells also enabled association of GCC88 with the TGN (Fig. 6, C and D). Finally, we found that, whereas the localization of endogenous ARFRP1 was not altered by ARL1 KO, endogenous ARL1 lost its TGN localization upon ARFRP1 KO (Fig. 6 E). These results were consistent with the decreased association of endogenous ARL1 with membranes in ARFRP1-KO cells analyzed by subcellular fractionation (Fig. 3, E and F). Therefore, ARFRP1 functions upstream of ARL1 to recruit GCC88 to the TGN.

Taken together, all of the above experiments indicated that ARFRP1 is the source of two GTPase cascades leading to the ARL5-dependent recruitment of GARP and ARL1-dependent recruitment of a subset of golgins to the TGN.

SYS1 regulates the ARFRP1-mediated recruitment of GARP to the TGN

The targeting of yeast Arl3p (ARFRP1 orthologue) to the late Golgi relies on acetylation of its N terminus and interaction with the transmembrane protein Sys1p (Behnia et al., 2004; Setty et al., 2004). To investigate if human SYS1 plays a similar role in the recruitment of ARFRP1, ARL1, GARP, and golgins, we examined the localization of these proteins in SYS1-KO HeLa cells (Fig. 7 A). We observed that KO of SYS1 caused dissociation of endogenous ARFRP1, ARL1, and GCC88 and transgenic VPS54-13Myc from the TGN (Fig. 7, B–F). The TGN localization of VPS54-13Myc and GCC88 could be restored by expression of GFP-tagged SYS1 in SYS1-KO cells (Fig. 7, C–F). Subcellular fractionation/immunoblotting experiments showed that SYS1 KO decreased the association of ARL5 as well as ARL1 and

ARFRP1 with membranes (Fig. 7, G and H). These decreases could be reversed by re-expression of SYS1 in the SYS1-KO cells (Fig. 7, G and H). Unexpectedly, we found that SYS1 KO also decreased the total amounts of ARFRP1 (Fig. 7, G and I), indicating that SYS1 stabilizes the ARFRP1 protein. In contrast to these effects, SYS1 KO did not affect the localization of the RAB6-dependent GCC185 and TMF1 golgins (Fig. S3). From these experiments, we concluded that SYS1 functions upstream of ARFRP1 to initiate the small GTPase cascades that lead to the recruitment of both golgins and GARP to the TGN.

Integrity of the TGN in KO cells

Finally, to ascertain that loss of localization of GARP, golgins, TGN46, and internalized Cy3-STxB to the TGN was not due to complete disappearance of this organelle in the various KO cells used in this study, we examined the localization of the TGN-associated adaptor protein Myc-GGA2 (Dell'Angelica et al., 2000), expressed by transient transfection in WT, ARL1-KO, ARL5-KO, ARFRP1-KO, RAB6-KO, and SYS1-KO cells (Fig. S4). We observed that Myc-GGA2 localized to the TGN in all these cell lines, although in some KO cells the TGN appeared slightly dispersed (Fig. S4). These results were consistent with the TGN association of GARP in ARL1-KO cells (Fig. 2 B), the TGN golgins in ARL5-KO cells (Fig. 5 A), and GCC185 in ARFRP1-KO (Fig. 5 A) and SYS1-KO cells (Fig. S3). Therefore, the KOs made in this study impaired the association of tethering factors and the retrograde transport of specific cargos to the TGN without fundamentally altering the integrity of this organelle.

Discussion

The results of our study demonstrate that SYS1 and ARFRP1 regulate not only the previously reported ARL1-dependent recruitment of a subset of golgins (Panic et al., 2003b; Setty et al., 2003; Shin et al., 2005; Zahn et al., 2006) but also the ARL5-dependent recruitment of GARP to the TGN (Fig. 8). SYS1 and ARFRP1 thus coordinate the recruitment of two structurally and functionally distinct classes of tethering factors to the TGN. This coordination likely ensures that the long-distance capture of retrograde transport carriers by the golgins is synchronized with the transfer of the carriers to GARP for their subsequent SNARE-dependent fusion with the TGN. The coordinated regulation of long coiled-coil tethers and MTCs enabled by this mechanism may be paradigmatic for other membrane fusion events that take place in the endomembrane system of eukaryotic cells.

The role of SYS1, ARFRP1, and ARL5 in the recruitment of GARP to the TGN

Previous studies of small GTPases that regulate the recruitment of GARP to the TGN in different organisms had painted a complicated picture involving RAB6, ARL1, ARL5, and their orthologues and paralogs (Siniossoglou and Pelham, 2001; Panic et al.,
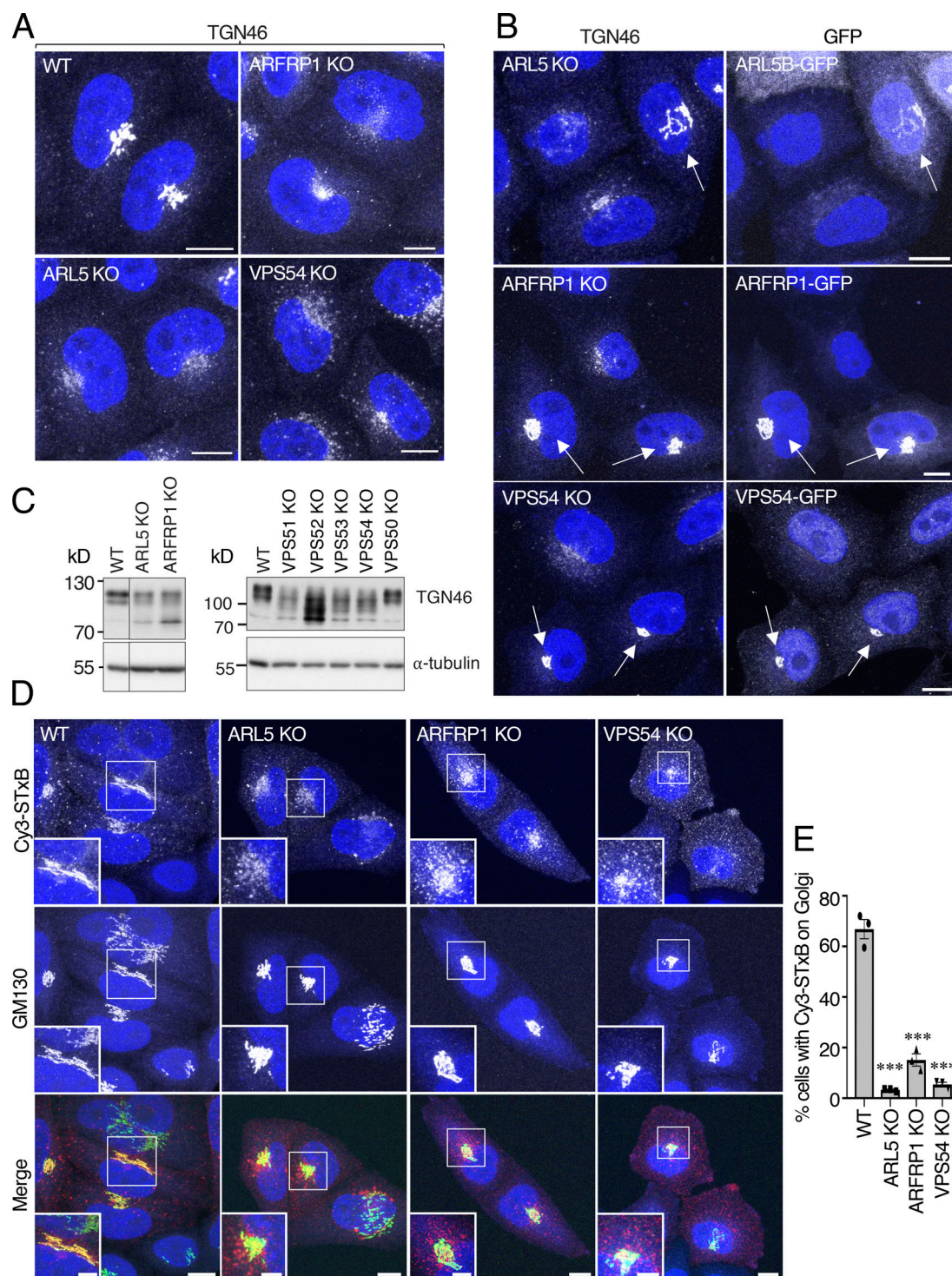
Figure 4. **Altered localization of TGN46 and impaired transport of STxB to the Golgi complex in ARL5-KO and ARFRP1-KO cells. (A)** Immunofluorescence microscopy of WT, ARFRP1-KO, ARL5-KO, and VPS54-KO cells immunostained for endogenous TGN46 and counterstained with DAPI (blue). Scale bars: 10 μm. **(B)** ARFRP1-KO, ARL5-KO, or VPS54-KO cells were rescued by expression of the corresponding GFP-tagged proteins, stained for endogenous TGN46, transgenic GFP (only for VPS54-GFP), and nuclei (DAPI; blue) and imaged by confocal microscopy (GFP fluorescence was directly observed for ARL5B-GFP and ARFRP1-GFP). Scale bars: 10 μm. Arrows indicate rescued cells. **(C)** SDS-PAGE and immunoblot analysis of endogenous TGN46 and α-tubulin (loading control) in WT and the indicated KO cells. The positions of molecular mass markers are indicated on the left. **(D)** Live WT, ARL5-KO, ARFRP1-KO, or VPS54-KO cells were incubated for 15 min with Cy3-STxB and chased for 1 h in regular culture medium at 37°C, after which cells were fixed, immunostained for endogenous GM130, and imaged by confocal microscopy. Scale bars: 10 μm. Insets are magnified views of the boxed areas. Inset scale bars: 5 μm. **(E)** Quantification of cells having Cy3-STxB staining at the TGN as described in Fig. 2 C. Values are the mean ± SEM from three independent experiments. More than 100 cells per sample were counted in each experiment. ***, P < 0.001, in comparison to WT cells using Dunnett's test.
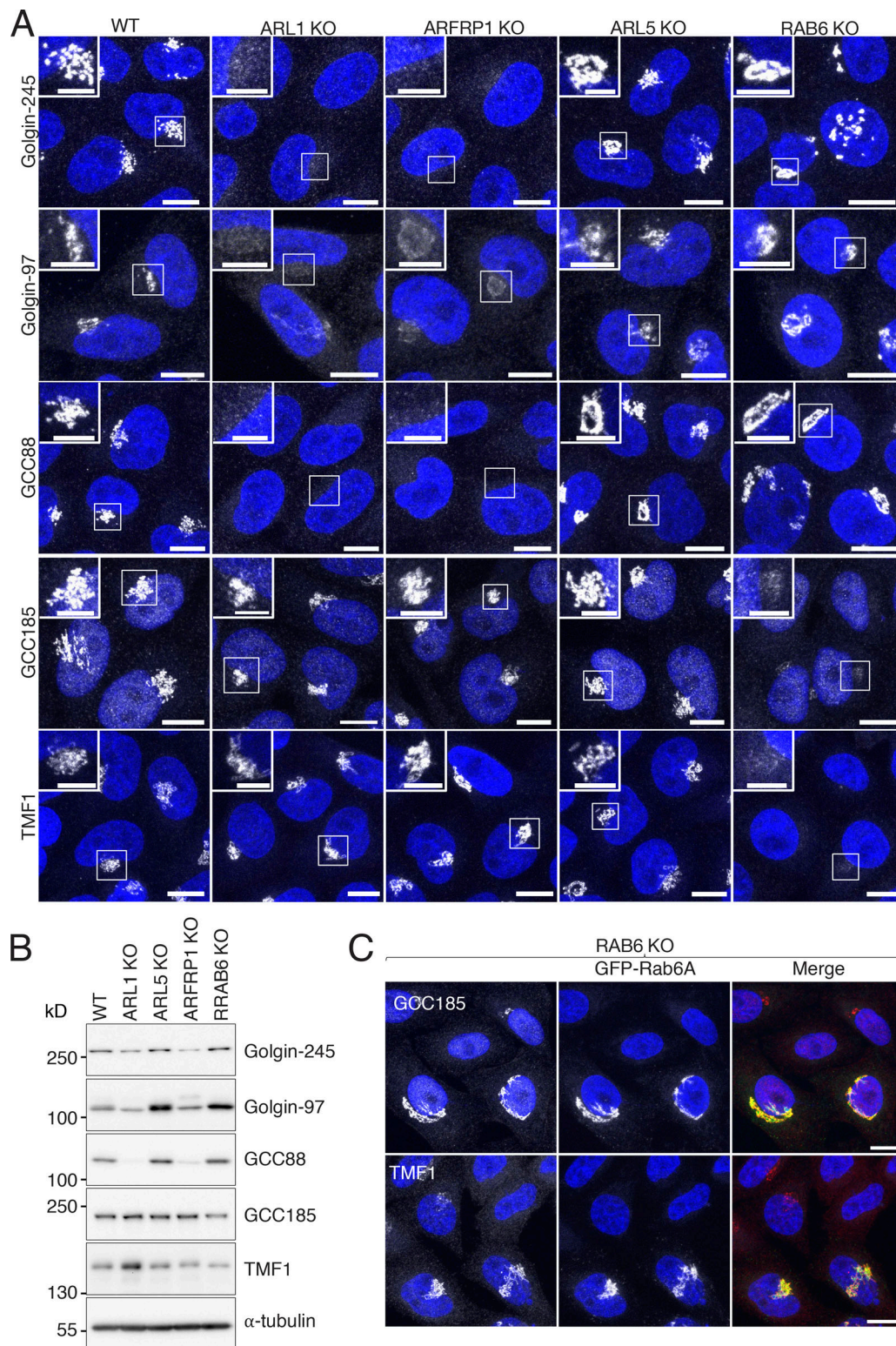
Figure 5. **Small GTPases required for localization of golgins to the TGN. (A)** Immunofluorescence microscopy of WT, ARL1-KO, ARFRP1-KO, ARL5-KO, and RAB6-KO cells immunostained for endogenous Golgin-245, Golgin-97, GCC88, GCC185, or TMF1 and counterstained with DAPI (blue). Scale bars: 10 μm. Insets are magnified views of the boxed areas. Inset scale bars: 5 μm. Notice that ARL1 KO or ARFRP1 KO caused complete disappearance of Golgin-245 and GCC88, and a partial decrease in the intensity of Golgin-97, at the TGN; quantification in 10 cells per sample in three independent experiment showed that Golgin-97 decrease was 75.6% ± 2.4% in ARL1-KO cells and 55.0% ± 1.9% in ARFRP1-KO cells. **(B)** SDS-PAGE and immunoblot analysis of endogenous golgins and α-tubulin (loading control) in WT and KO cells. The positions of molecular mass markers are indicated on the left. **(C)** Immunofluorescence microscopy of RAB6-KO cells transfected with a plasmid encoding GFP-tagged mouse Rab6A (green), immunostained for endogenous GCC185 and TMF1 (red), and counterstained with DAPI (blue). Cells were examined for GFP fluorescence by confocal microscopy. Scale bars: 10 μm.
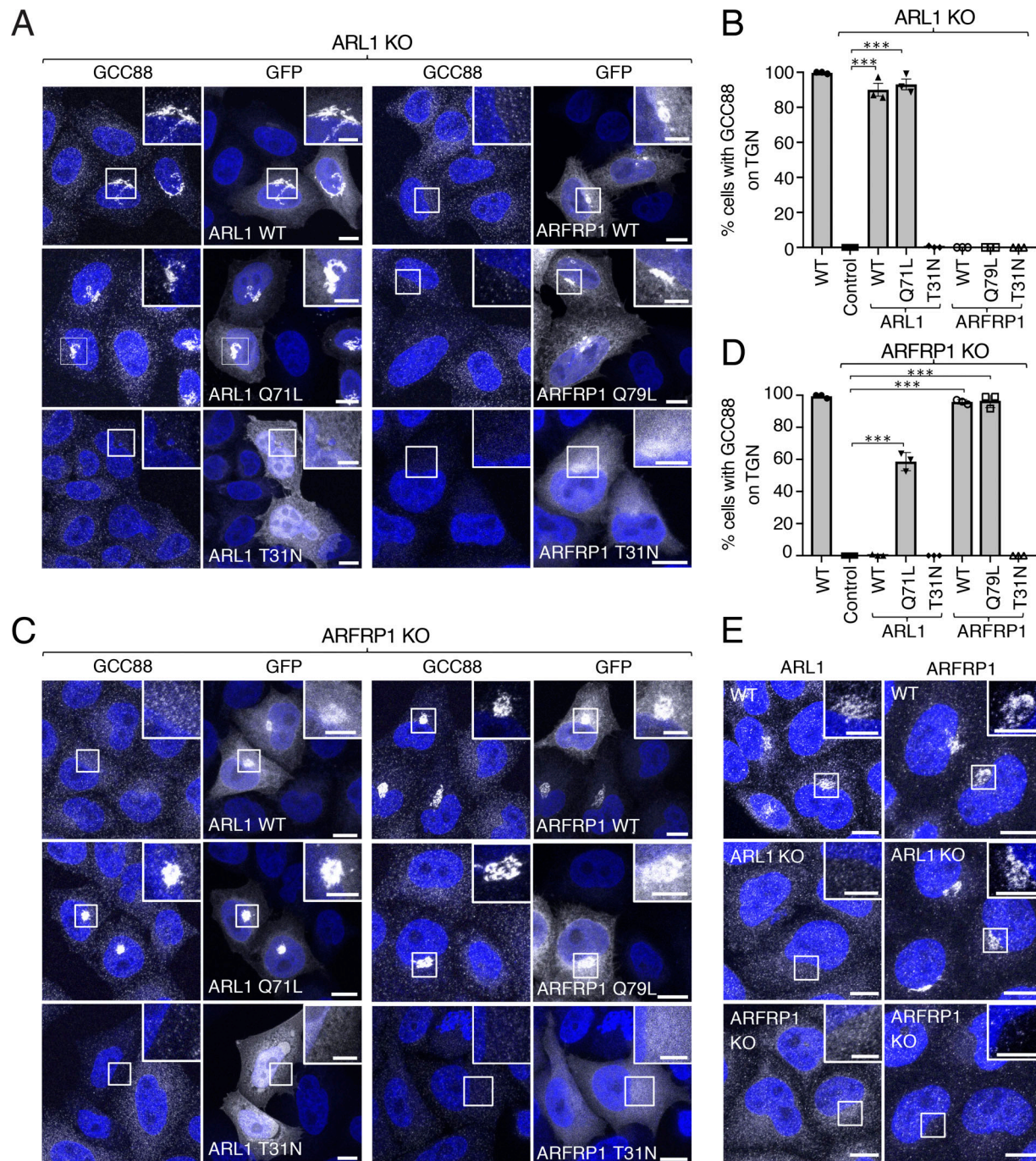
Figure 6. **ARFRP1 functions upstream of ARL1 in the recruitment of GCC88 to the TGN. (A)** ARL1-KO cells were transfected with plasmids encoding GFP-tagged ARL1 (WT, Q71L, or T31N) or GFP-tagged ARFRP1 (WT, Q79L, or T31N), immunostained for endogenous GCC88, counterstained with DAPI (blue), and imaged by confocal microscopy. **(B)** The percentage of cells having GCC88 staining at the TGN from experiments such as that in panel A was quantified as described in Fig. 2 C. Values are the mean ± SEM from three independent experiments. More than 100 cells per sample were counted in each experiment. ***, P < 0.001, in comparison to untransfected ARL1 KO cells using Dunnett's test. **(C)** ARFRP1-KO cells were transfected and analyzed as described in A. **(D)** The percentage of cells having GCC88 staining at the TGN from experiments such as that in C was quantified as described in Fig. 2 C. Values are the mean ± SEM from three independent experiments. More than 100 cells per sample were counted in each experiment. ***, P < 0.001, in comparison to untransfected ARFRP1 KO cells using Dunnett's test. **(E)** WT, ARL1-KO, or ARFRP1-KO cells were immunostained for endogenous ARL1 or ARFRP1, counterstained with DAPI (blue), and imaged by confocal microscopy. Scale bars: 10 µm. Insets are magnified views of the boxed areas. Inset scale bars: 5 µm.

2003b; Liewen et al., 2005; Rosa-Ferreira et al., 2015). Following on the finding that RAB4 may regulate the recruitment of the related EARP complex to endosomes (Gillingham et al., 2014; Schindler et al., 2015), we spent considerable effort performing

siRNA and dominant-negative interference screens to identify RAB GTPases that mediate the recruitment of GARP to the TGN. This effort, however, failed to produce any reliable hits. We thus switched our approach to testing for the role of ARL-family
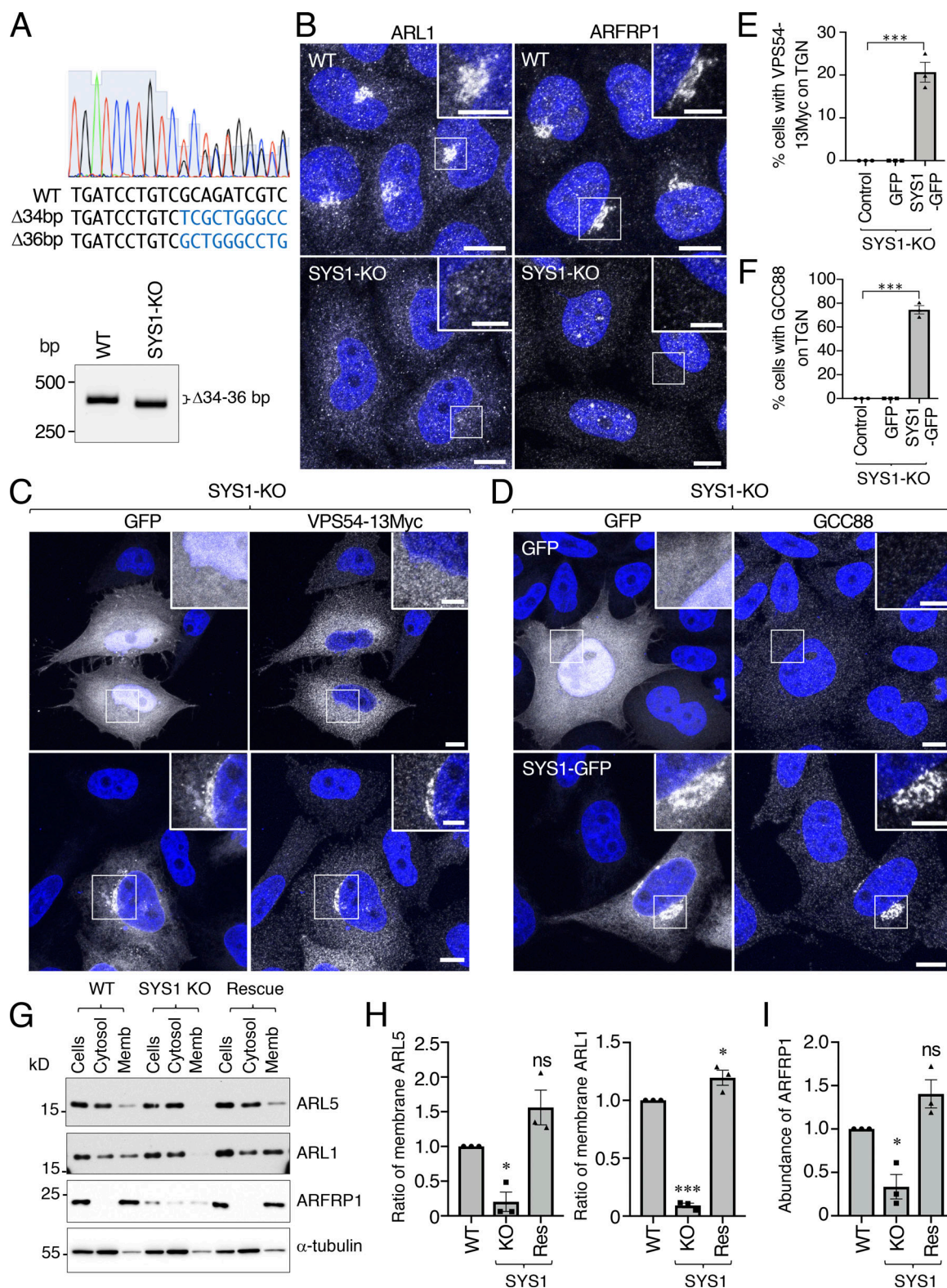
Figure 7. **SYS1 is required for the association of ARFRP1, ARL1, GCC88, and GARP with the TGN. (A)** Due to the lack of good antibodies to SYS1, KO of the *SYS1* gene was demonstrated by Sanger sequencing (top) and genomic PCR (bottom). KO resulted in a 34- and 36-bp deletion. The 34-bp deletion is predicted to result in a frameshift causing premature termination at amino acid 28. The 36-bp deletion is not predicted to result in a frameshift, but to cause a deletion of more than half of the first transmembrane domain. **(B)** WT and SYS1-KO cells were immunostained for endogenous ARL1 or ARFRP1, counterstained with DAPI (blue), and imaged by confocal microscopy. **(C)** SYS1-KO cells were co-transfected with plasmids encoding VPS54-13Myc and either GFP alone or SYS1-GFP as indicated in the figure, immunostained for the Myc epitope, counterstained with DAPI (blue), and imaged by confocal microscopy. Insets are magnified views of the boxed areas. Inset scale bars: 5 µm. **(D)** SYS1-KO cells were transfected with plasmids encoding GFP or SYS1-GFP as indicated in the figure, immunostained

for endogenous GCC88, counterstained with DAPI (blue), and imaged by confocal microscopy. Scale bars in B, C, and D: 10 μm. **(E)** Quantification of cells having VPS54-13Myc staining at the TGN as described in Fig. 2 C. Values are the mean ± SEM from three independent experiments. More than 100 cells per sample were counted in each experiment. **(F)** Quantification of cells having GCC88 staining at the TGN as described in Fig. 2 C. Values are the mean ± SEM from three independent experiments. More than 100 cells per sample were counted in each experiment. In E and F, the statistical significance of the differences relative to SYS1-KO cells only expressing VPS54-13Myc (control; E) or untransfected SYS1-KO cells (F) was determined using Dunnett's test. ***, $P < 0.001$. **(G)** Subcellular fractionation of WT, SYS1-KO, and SYS1-rescue (Res) HeLa cells performed as described in Fig. 3 E. **(H)** The ratio of membrane to the sum of membrane and cytosolic ARL1 and ARL5 protein from the experiments described in G was quantified as described in Fig. 3 F. Values are the mean ± SEM from three independent experiments. *, $P < 0.05$; ***, $P < 0.001$. **(I)** Quantification of the abundance of ARFRP1 normalized to the abundance of α-tubulin from the experiments described in G. Band intensities in whole cells were measured, and values for SYS1-KO cells and SYS1-rescue cells were normalized to WT cells. Values are the mean ± SEM from three independent experiments. The statistical significance of the differences relative to WT cells was determined using Dunnett's test. *, $P < 0.05$.

GTPases using CRISPR/Cas9 KO cells. This approach succeeded in revealing that ARL5, but not ARL1 and RAB6, is required for GARP recruitment to the TGN in human cells. The effect of ARL5 KO was more complete than that of ARL5 KD used in previous studies
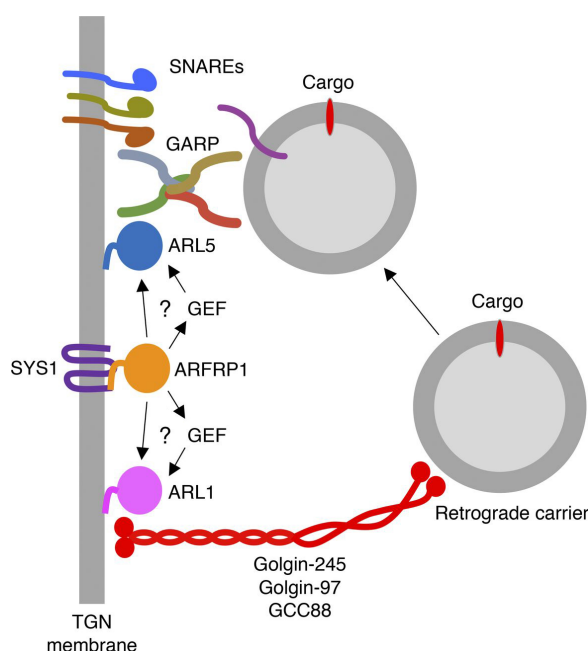

Figure 8. **Model for the function of ARFRP1 in the coordinated recruitment of golgins and GARP to the TGN.** This model is based on results shown in this article and previous publications cited in the text. The multispanning membrane protein SYS1 recruits ARFRP1 to the TGN, possibly by acting as a GEF that converts ARFRP1-GDP to ARFRP1-GTP. This process involves the N-terminally acetylated amphipathic α-helix of ARFRP1. ARFRP1 then promotes the recruitment and/or activation of both ARL1 and ARL5 to the TGN. ARFRP1 could do so either by acting as a GEF or by recruiting specific GEFs for ARL1 or ARL5. The resulting ARL1-GTP and ARL5-GTP associate with the TGN membrane via their N-terminally myristoylated amphipathic α-helices. ARL1 in turn recruits three golgins to the TGN (Golgin-245, Golgin-97, and GCC88), which capture retrograde transport carriers containing specific cargos. ARL5, on the other hand, recruits the GARP complex. The golgins then undergo a conformational collapse (Cheung et al., 2015) that brings the carriers close to the TGN, enabling the transfer of the carriers to GARP. Finally, GARP promotes the assembly of the trans-SNARE complex that allows fusion of the carrier and TGN membranes, resulting in delivery of the specific cargos to the TGN. SYS1 and ARFRP1 thus function upstream of two other small GTPases, enabling the recruitment of distinct types of tethering factors to the TGN. A fourth golgin, GCC185, is recruited to the TGN by RAB6. It remains to be determined if and how RAB6-GCC185 coordinates with ARFRP1-ARL5-GARP to tether transport carriers to the TGN.

(Rosa-Ferreira et al., 2015), providing strong confirmation that this GTPase is critical for GARP recruitment to the TGN. The fact that Drosophila ARL5 physically interacts with GARP (Rosa-Ferreira et al., 2015) makes it likely that GARP is a direct effector of ARL5.

A surprising finding was that a second ARL-family GTPase, ARFRP1, was also required for GARP recruitment to the TGN. This GTPase had previously been shown to localize to the TGN and to mediate both forward and retrograde transport processes at this organelle (Shin et al., 2005; Zahn et al., 2008; Nishimoto-Morita et al., 2009; Guo et al., 2013; Ma et al., 2018). Most importantly for our study, ARFRP1 and its yeast orthologue Arl3p had been shown to mediate recruitment of ARL1/Arl1p and their effector golgins to the TGN (Panic et al., 2003b; Setty et al., 2003; Shin et al., 2005; Zahn et al., 2006). This raised the possibility that ARFRP1 could similarly function upstream of ARL5 to recruit GARP to the TGN. Indeed, we found that ARFRP1-KO decreased the association of ARL5 with membranes and that the dissociation of GARP from the TGN in ARFRP1-KO cells could be suppressed by overexpression of constitutively active but not inactive ARL5, indicating that ARFRP1-GTP is required for activation of ARL5. Since yeast Sys1p had been shown to target Arl3p to the late Golgi (Behnia et al., 2004; Setty et al., 2004), we also tested whether the orthologous human SYS1 was required for ARFRP1 recruitment to the TGN. We found that not only was this the case, but also that SYS1 was required for ARL1, ARL5, GCC88, and GARP recruitment to the TGN. Moreover, we observed that SYS1 was required for the maintenance of normal levels of ARFRP1, suggesting that formation of a complex between SYS1 and ARFRP1 stabilizes the ARFRP1 protein. The SYS1-ARFRP1 ensemble thus regulates both the ARL1-golgin and ARL5-GARP arms of vesicle tethering at the TGN (Fig. 8).

Small GTPases that regulate the recruitment of golgins to the TGN

The Arl3p-Arl1p arm is well known to regulate the recruitment of the only GRIP domain–containing golgin in yeast, Imh1p (Panic et al., 2003b; Setty et al., 2003). Similarly, there is agreement that ARFRP1 and ARL1 regulate the recruitment of Golgin-245 and Golgin-97 to the TGN (Lu and Hong, 2003; Derby et al., 2004; Wu et al., 2004; Shin et al., 2005; Zahn et al., 2006). In addition to confirming these findings, we observed that association of GCC88 with the TGN is dependent on both ARFRP1 and ARL1, but not ARL5 and RAB6. There is less agreement in the literature about the specific GTPase requirement for recruitment of GCC185 to the TGN. Whereas one study showed that ARL1 and RAB6A/A′ (splice variants of RAB6A) cooperate to recruit

GCC185 to the TGN (Burguete et al., 2008), another study argued that the localization of GCC185 to the TGN is independent of both ARL1 and RAB6A/A′ (Houghton et al., 2009). Our analyses using KO cells now demonstrate that GCC185 recruitment to the TGN is independent of ARFRP1, ARL1, and ARL5, but dependent on RAB6. The difference with previous studies could be due to the KO of RAB6B in addition to RAB6A in our study. Our results lead us to conclude the existence of two distinct mechanisms for the recruitment of golgins to the TGN: ARFRP1-ARL1 for Golgin-245, Golgin-97, and GCC88, and RAB6 for GCC185. Although these are the predominant mechanisms, we cannot rule out that other small GTPases contribute to some extent to the recruitment or function of these TGN golgins. The existence of cooperative or alternative mechanisms for tethering to the TGN is supported by the ability to suppress defects in yeast Arl1p mutants by overexpression of Ypt6p (Wakade et al., 2017) and vice versa (Chen et al., 2019).

How does ARFRP1 mediate recruitment and function of ARL5 and ARL1?

A plausible explanation for the functional relationships among the ARL GTPases examined in our study is that ARFRP1 functions as a guanine nucleotide exchange factor (GEF) for exchange of GTP for GDP on both ARL5 and ARL1. A precedent for such a mechanism is the activity of ARL13B as a GEF for ARL3 in the process of ciliogenesis (Gotthardt et al., 2015; Ivanova et al., 2017). However, ARL13B is atypical in that, in addition to its G-domain, it comprises an ~20-kD C-terminal extension that is required for its ARL3-GEF activity and that is not present in ARFRP1. An alternative explanation would be that ARFRP1 recruits GEFs for ARL5 and ARL1. This would be analogous to the role of the yeast RAB Ypt32p in recruiting the Sec4p GEF for another RAB, Sec2p (Ortiz et al., 2002), and of the mammalian RAB33B in recruiting the RIC1-RGP1 GEF for RAB6A (Pusapati et al., 2012). Yeast Mon2p was proposed to act as a GEF for Arl1p (Jochum et al., 2002) and to function together with Arl3p and Arl1p in an alternative pathway to that mediated by Ypt6p (Setty et al., 2003). However, KO of MON2 did not affect Arl1p and Imh1p recruitment to the late Golgi (Panic et al., 2003b; Setty et al., 2003). To date, no other candidate GEFs for ARL5 and ARL1 have been identified. Further studies will thus be required to determine whether ARFRP1 has intrinsic GEF activity toward ARL5 and ARL1, or whether it functions to recruit distinct GEFs for these ARLs.

In addition to elucidating a mechanism that enables the coordinated regulation of two types of vesicle-tethering factor, our findings have uncovered a novel principle in which a single small GTPase is the origin of two small GTPase cascades involved in protein trafficking. As GEFs and GAPs for other small GTPases are identified, it will be of interest to determine if a similar principle applies to other vesicle-tethering events or to other trafficking processes that depend on simultaneous engagement of distinct sets of proteins by multiple small GTPases.

Materials and methods
Antibodies
The following antibodies were used for immunoblotting and/or immunofluorescence microscopy: rabbit anti-VPS51 (HPA039650;

Atlas Antibodies), rabbit anti-VPS52 made in our laboratory (Pérez-Victoria et al., 2008), rabbit anti-VPS53 (HPA024446; Atlas Antibodies), mouse anti-VPS50 (FLJ20097, monoclonal antibody M01, 2D11; Abnova), mouse anti-Myc epitope (9E10; Santa Cruz Biotechnology), sheep anti-TGN46 (AHP500G; Bio-Rad), mouse anti–β-actin (G043; Applied Biological Materials), rabbit anti-giantin (ab80864; Abcam), mouse HRP-conjugated anti-α-tubulin (DM1A; Santa Cruz Biotechnology), rabbit anti-ARL1 (16012-1-AP; Proteintech), rabbit anti-ARFRP1 (PA5-50606; Thermo Fisher Scientific), mouse anti-ARL5A (sc-514680; Santa Cruz Biotechnology), rabbit anti-RAB6A (GTX110646; GeneTex), rabbit anti-GCC88 (HPA021323; Sigma-Aldrich), rabbit anti-GCC185 (HPA035849; Sigma-Aldrich), mouse anti-Golgin-245 (611281; BD Biosciences), mouse anti-GM130 (610822; BD Biosciences), mouse anti–Golgin-97 (A-21270; Thermo Fisher Scientific), rabbit anti-TMF1 (HPA008729, Sigma-Aldrich), monoclonal HRP-conjugated anti-GFP (Miltenyi Biotec Inc.), rabbit anti-GFP (A-11122; Thermo Fisher Scientific), HRP-conjugated goat anti-rabbit and donkey anti-mouse antibodies (Jackson ImmunoResearch), HRP-conjugated donkey anti-sheep (R&D Systems), and Alexa Fluor–conjugated secondary antibodies for immunostaining (Thermo Fisher Scientific).

Plasmid constructs
A plasmid encoding human VPS54 with a C-terminal 13Myc tag (pCI-neo-hVPS54-13Myc) was described previously (Gershlick et al., 2019). Human VPS54 cDNA was purchased (Origene) and subcloned into the pEGFP-N1 vector (Clontech, Takara Bio Inc.). The purchased VPS54 cDNA contains a 120-bp insertion at the 3′ coding region (5′-ACAGGGTCTCATGGTCACACAGGCTGGAGGGCAGTGGTGTGATCATGGCTCACTGCAGCCTCAACCTCCGTGGCTCAAGCAATCCTCCCACTGCAGACTCCCCAATAACTGCGACTACAG-3′) that is likely to derive from alternative splicing. As a result, 40 amino acids (QGLMVTQAGGQWCDHGSLQPQPPWLKQSSHCRLPNNCDYR) are inserted after Gly943 of the human VPS54 sequence registered in UniProt (Q9P1Q0). Sequences encoding N-terminal (amino acid residues 1–557) and C-terminal halves (amino acid residues 558–1,017) of VPS54 were amplified and subcloned into a pCI-neo-13Myc backbone vector (Schindler et al., 2015). Human ARL5B (#67400) and ARFRP1 (#67471) cDNAs were obtained from Addgene (deposited by Richard Kahn, Emory University, Atlanta, GA) and subcloned into pEGFP-N1. The ARFRP1 cDNA was also subcloned into a pQCXIP vector (Clontech). Constitutively active and inactive forms of ARL1, ARL5B, and ARFRP1 tagged with EGFP (herein referred to as GFP) were generated by site-directed mutagenesis using Q5 High-Fidelity DNA Polymerase (New England Biolabs). pGFP-C1-mouse Rab6A and Rab6B were the kind gift of Mitsunori Fukuda (Tohoku University, Sendai, Japan; Matsui et al., 2011). Human SYS1 cDNA was obtained from the ORFeome v8.1 collection (Dharmacon) and subcloned into the pGFP-N1 and pQCXIP vectors. A plasmid encoding Myc-GGA2 (pCR3.1-Myc-hGGA2) was previously described (Dell'Angelica et al., 2000). The sequence of all constructs was confirmed by Sanger sequencing.

siRNAs
The following FlexiPlate siRNAs (Qiagen) were used in our experiments: human ARL5A (5′-CAAGTTAATGGCATTGATTTA/CACGTTTCCTAATGTGGGATA-3′), human ARL5B (5′-CTCCCG

GATTGGTGTGAGATA/CTGCCTTCTTGTATCTAGTAA-3′), human RAB6A (5′-CAGATGGGTCATATTCTTTAT/TACGGTCTTCTTTGA GGTCAA-3′), human RAB6B (5′-CGGCTGTTACTTAAACAACTA/ ATCCATGTTCTTAGAGCCTCA-3′). Control siRNA (5′-CAGTCG CGTTTGCGACTGGTT-3′) was purchased from Dharmacon.

CRISPR/Cas9 KO

VPS50-KO, VPS51-KO, VPS52-KO, VPS53-KO, VPS54-KO, ARL1-KO, ARL5-KO, ARFRP1-KO, RAB6-KO, and SYS1-KO HeLa cells were generated using CRISPR/Cas9 (Cong et al., 2013). The targeting sequences for VPS50 (5′-TGAACAAGTATATTTTTC TG/TGATATTGTTAAATATGAGC/ATAAGCTCTTGTTCAGCT TG-3′), VPS51 (5′-CCTAGCCCGGGGTCTGGACC/TGCGCCTTC CGCCGACGCTC/TCGCATCAGCGCCACGCTGC/CGTCACCCTCCG TCCCCCAG-3′), VPS52 (5′-CTCTGAGATCCGGACACTGC/TGG GGAGCTTGTTGATGGTC-3′), VPS53 (5′-GGAGGAGGAACTGGA GTTCG/GGTGCAGCTGGCCATCGAGC-3′), VPS54 (5′-ACTGCC AGATGTGTGTCCCA/GAGGCACTGGTGAAGAACTG-3′), ARL1 (5′-TTTCCAGTCTGTTTGGAACT/TTGTAATCTGTACAAAATTG-3′), ARL5A (5′-TAATACACGTTTCCTAATGT/CACTTACTATAC TAACACAG-3′), ARL5B (5′-CAAAGTAATTATAGTGGGAC/TAA ACACCCATACTTACAAT-3′), ARFRP1 (5′-TCCTGGGCCTGGACA ATGCT/GTACAAGTACATGTTTCAGA-3′), RAB6A (5′-ATGTCC ACGGGCGGAGACTT/GGAGCAAAGCGGTGAGTGCG-3′), RAB6B (5′-ATGTCCGCAGGGGGAGATTT/TTGGGCGGCGGGGGTCGA CT-3′), and SYS1 (5′-ACCGTGTATTACGGCTCGCT/GCATGAGGA CGATCTGCGAC-3′) were cloned separately into pSpCas9 (BB)-2A-GFP plasmid (#48138; Addgene; deposited by Feng Zhang, Massachusetts Institute of Technology, Cambridge, MA). HeLa cells were transfected with two to four plasmids containing the different targeting sequences for the same gene, and GFP-positive cells were isolated by flow cytofluorometry after 24 h and single-cell cloned in 96-well plates. KO of each clone was confirmed by immunoblotting using specific antibodies. Because we were not able to obtain antibodies that detect VPS54 and SYS1, we confirmed genomic deletions in these genes by Sanger sequencing of the genomic PCR products. The following primers were used to amplify each fragment: VPS54, 5′-TCAATTTTCCCA ATTAAGAGCAA-3′ (forward), 5′-CACCATGTTAGCCAGGATGA-3′ (reverse); SYS1, 5′-GACTCTTGGAATGGGCTCAC-3′ (forward), 5′-TTCCCAGGGCTACAAAGAAA-3′ (reverse). To generate ARFRP1-rescue and SYS1-rescue cells, retrovirus particles were prepared by transfecting HEK293T cells with pQCXIP-ARFRP1 or pQCXIP-SYS1 and retrovirus packaging plasmids (Clontech). Medium was collected 48 h after transfection and centrifuged for 10 min at 1,000 ×g to remove debris. The ARFRP1-KO or SYS1-KO HeLa cells were immediately infected with the corresponding virus, and stably transduced cells were selected with 2 µg/ml puromycin.

Cell culture and transfection

Unless otherwise specified, most experiments were done in HeLa cells (ATCC). H4 and HEK293T cells (ATCC) were used in some experiments. All cells were cultured in DMEM supplemented with 10% FBS and MycoZap Plus-CL (Lonza). Plasmids were transfected using Lipofectamine 2000 (Thermo Fisher Scientific), and cells were analyzed 24–48 h after transfection.

siRNAs were transfected with Lipofectamine RNAiMAX (Thermo Fisher Scientific), and cells were analyzed 72 h after transfection.

Immunoblot analysis

Cells were scraped off the dish and lysed in buffer containing 1% Triton X-100; 50 mM Tris, pH 7.4; 150 mM NaCl; and cOmplete EDTA-free Protease Inhibitor (Roche). Laemmli SDS-PAGE sample buffer (Bio-Rad) containing 2.5% 2-mercaptoethanol was added to the lysate and incubated for 5 min at 98°C. Immunoblotting was performed using SDS-PAGE separation and subsequent transfer to polyvinyl difluoride or nitrocellulose membranes. Membranes were blocked for 0.5–1 h with 3% nonfat milk (Bio-Rad) in TBS-T (TBS supplemented with 0.05% Tween 20; Sigma-Aldrich) before being incubated overnight with primary antibody diluted in TBS-T with 3% nonfat milk. Membranes were washed three times for 20 min in TBS-T before being incubated for 2–3 h in HRP-conjugated secondary antibody (1:5,000) diluted in TBS-T with 3% nonfat milk. Membranes were washed three times in TBS-T and visualized using either Clarity ECL Western Blot substrate (Bio-Rad) or a 1:1 mixture of homemade ECL solution (Solution 1: 0.25 mM luminol, 0.37 mM p-coumaric acid, and 0.1 M Tris–HCl, pH 8.5; and Solution 2: 0.0192% hydrogen peroxide and 0.1 M Tris-HCl, pH 8.5).

Immunofluorescent staining

Cells for immunofluorescence microscopy were plated onto fibronectin-coated cover glasses, transfected as described above, and fixed using 4% paraformaldehyde in PBS. Cells were permeabilized with 0.1% Triton-X in PBS at RT for 5 min and incubated in blocking buffer (1% BSA in PBS) for 30 min. Primary antibodies were diluted in blocking buffer and incubated on cells for 1 h at RT. Alexa Fluor secondary antibodies were diluted in blocking buffer containing DAPI, and cells were incubated for 1 h at RT. The coverslips were mounted on glass slides using ProLong Gold Antifade (Thermo Fisher Scientific), and the cells were imaged on a confocal microscope (LSM710 or LSM880; Carl Zeiss) with an oil-immersion 63×/1.40 NA Plan-Apochromat Oil DIC M27 objective lens (Carl Zeiss). Image settings (i.e., gain, laser power, and pinhole) were kept constant for images presented for comparison. Images were acquired using ZEN 2012 software (Carl Zeiss) and processed by Fiji (https://fiji.sc), including brightness adjustment, contrast adjustment, channel merging, and cropping.

Uptake of STxB

Uptake of Cy3-STxB (Amessou et al., 2006; kind gift of David Gershlick, University of Cambridge, Cambridge, UK) was performed as previously described (Pérez-Victoria et al., 2008). Briefly, cells were incubated for 30 min in STxB uptake medium (DMEM without FBS plus 1% BSA). Cells were subsequently incubated with 0.5 µg/ml Cy3-STxB in STxB uptake medium for 15 min and washed with PBS once before being incubated for 1 h with prewarmed complete DMEM. Cells were then fixed with 4% paraformaldehyde in PBS and immunostained for GM130 as a marker for the Golgi complex as described above.

Cytosol-membrane fractionation

A cell fractionation kit (#9038; Cell Signaling Technology) was used to fractionate proteins into cytosolic and membrane fractions according to the manufacturer's instructions. Briefly, cells on a culture dish were trypsinized, and 2.5 million cells were aliquoted into a 1.5-ml tube. Cells were washed with PBS once and resuspended in 0.5 ml PBS. 0.1 ml of the suspension was aliquoted into another 1.5-ml tube for analysis of whole-cell lysate. The rest of the suspension was centrifuged for 5 min at 500 ×*g* at 4°C, and the pellet was resuspended in 0.5 ml of cytoplasmic isolation buffer. After incubation on ice for 5 min, the suspension was centrifuged for 5 min at 500 ×*g* at 4°C, and the supernatant was saved as the cytosolic fraction. The pellet was resuspended in 0.5 ml of membrane isolation buffer and incubated on ice for 5 min. The suspension was centrifuged for 5 min at 8,000 ×*g* at 4°C. The supernatant was saved as the membrane fraction. Laemmli sample buffer (Bio-Rad) containing 2.5% 2-mercaptoethanol was added to each fraction, and all samples were heated for 5 min at 98°C. Samples were subjected to SDS-PAGE followed by immunoblotting as described above.

Quantification and statistics

Quantification of the percentage of cells with VPS54-13Myc (Fig. 2 C; Fig. 3, B and D; and Fig. 7 E), Cy3-StxB (Fig. 4 E), or GCC88 (Fig. 6, B and D; and Fig. 7 F) on the TGN was performed by counting >100 cells per experiment per sample in three independent experiments. Percentages were calculated with Excel (Microsoft) and, wherever indicated, statistically analyzed by Dunnett's multiple comparison test (Prism 8 for macOS; GraphPad Software). Quantification of the ratio of membrane to the sum of membrane and cytosolic ARL1 and ARL5 in subcellular fractionation experiments (Fig. 3 F and Fig. 7 H), the protein abundance of ARFRP1 (Fig. 7 I), and the mean intensity of Golgin-97 after background subtraction in immunofluorescent images (Fig. 5 A) was performed in Fiji. Percentages were calculated with Excel (Microsoft) and statistically analyzed by Dunnett's multiple comparison test (Prism 8 for macOS). All quantitative data are expressed as the mean ± SEM, and all graphs were drawn using Prism 8 for macOS. Asterisks indicate the calculated statistical significance, as follows: NS, $P > 0.05$; *, $P \leq 0.05$; **, $P \leq 0.01$; ***, $P \leq 0.001$.

Online supplemental material

Fig. S1 shows validation of epitope-tagged VPS54 as a surrogate for GARP in immunofluorescence microscopy experiments. Fig. S2 shows specificity of antibodies to ARL5 and RAB6 paralogs. Fig. S3 shows intracellular localization of GCC185 and TMF1 in WT and SYS1-KO cells. Fig. S4 shows intracellular localization of Myc-GGA2 in WT, ARL1-KO, ARL5-KO, ARFRP1-KO, RAB6-KO, and SYS1-KO cells.

Acknowledgments

References

Amessou, M., V. Popoff, B. Yelamos, A. Saint-Pol, and L. Johannes. 2006. Measuring retrograde transport to the trans-Golgi network. *Curr. Protoc. Cell Biol.* Chapter15:15.10.

Behnia, R., B. Panic, J.R. Whyte, and S. Munro. 2004. Targeting of the Arf-like GTPase Arl3p to the Golgi requires N-terminal acetylation and the membrane protein Sys1p. *Nat. Cell Biol.* 6:405–413. https://doi.org/10.1038/ncb1120

Bennett, D., and L.C. Dunn. 1958. Effects on embryonic development of a group of genetically similar lethal alleles derived from different populations of wild house mice. *J. Morphol.* 103:135–157. https://doi.org/10.1002/jmor.1051030106

Bonifacino, J.S., and A. Hierro. 2011. Transport according to GARP: Receiving retrograde cargo at the trans-Golgi network. *Trends Cell Biol.* 21:159–167. https://doi.org/10.1016/j.tcb.2010.11.003

Burguete, A.S., T.D. Fenn, A.T. Brunger, and S.R. Pfeffer. 2008. Rab and Arl GTPase family members cooperate in the localization of the golgin GCC185. *Cell.* 132:286–298. https://doi.org/10.1016/j.cell.2007.11.048

Chen, Y.T., I.H. Wang, Y.H. Wang, W.Y. Chiu, J.H. Hu, W.H. Chen, and F.S. Lee. 2019. Action of Arl1 GTPase and golgin Imh1 in Ypt6-independent retrograde transport from endosomes to the trans-Golgi network. *Mol. Biol. Cell.* 30:1008–1019. https://doi.org/10.1091/mbc.E18-09-0579

Cheung, P.Y., and S.R. Pfeffer. 2016. Transport vesicle tethering at the trans Golgi network: Coiled coil proteins in action. *Front. Cell Dev. Biol.* 4:18. https://doi.org/10.3389/fcell.2016.00018

Cheung, P.Y., C. Limouse, H. Mabuchi, and S.R. Pfeffer. 2015. Protein flexibility is required for vesicle tethering at the Golgi. *eLife.* 4:e12790. https://doi.org/10.7554/eLife.12790

Cong, L., F.A. Ran, D. Cox, S. Lin, R. Barretto, N. Habib, P.D. Hsu, X. Wu, W. Jiang, L.A. Marraffini, et al. 2013. Multiplex genome engineering using CRISPR/Cas systems. *Science.* 339:819–823. https://doi.org/10.1126/science.1231143

Conibear, E., J.N. Cleck, and T.H. Stevens. 2003. Vps51p mediates the association of the GARP (Vps52/53/54) complex with the late Golgi t-SNARE Tlg1p. *Mol. Biol. Cell.* 14:1610–1623. https://doi.org/10.1091/mbc.e02-10-0654

Dell'Angelica, E.C., R. Puertollano, C. Mullins, R.C. Aguilar, J.D. Vargas, L.M. Hartnell, and J.S. Bonifacino. 2000. GGAs: A family of ADP ribosylation factor-binding proteins related to adaptors and associated with the Golgi complex. *J. Cell Biol.* 149:81–94. https://doi.org/10.1083/jcb.149.1.81

Derby, M.C., C. van Vliet, D. Brown, M.R. Luke, L. Lu, W. Hong, J.L. Stow, and P.A. Gleeson. 2004. Mammalian GRIP domain proteins differ in their membrane binding properties and are recruited to distinct domains of the TGN. *J. Cell Sci.* 117:5865–5874. https://doi.org/10.1242/jcs.01497

Derby, M.C., Z.Z. Lieu, D. Brown, J.L. Stow, B. Goud, and P.A. Gleeson. 2007. The trans-Golgi network golgin, GCC185, is required for endosome-to-Golgi transport and maintenance of Golgi structure. *Traffic.* 8:758–773. https://doi.org/10.1111/j.1600-0854.2007.00563.x

Donaldson, J.G., and C.L. Jackson. 2011. ARF family G proteins and their regulators: Roles in membrane transport, development and disease. *Nat. Rev. Mol. Cell Biol.* 12:362–375. https://doi.org/10.1038/nrm3117

Feinstein, M., H. Flusser, T. Lerman-Sagie, B. Ben-Zeev, D. Lev, O. Agamy, I. Cohen, R. Kadir, S. Sivan, E. Leshinsky-Silver, et al. 2014. VPS53 mutations cause progressive cerebello-cerebral atrophy type 2 (PCCA2). *J. Med. Genet.* 51:303–308. https://doi.org/10.1136/jmedgenet-2013-101823

Fridmann-Sirkis, Y., S. Siniossoglou, and H.R. Pelham. 2004. TMF is a golgin that binds Rab6 and influences Golgi morphology. *BMC Cell Biol.* 5:18. https://doi.org/10.1186/1471-2121-5-18

Gershlick, D.C., M. Ishida, J.R. Jones, A. Bellomo, J.S. Bonifacino, and D.B. Everman. 2019. A neurodevelopmental disorder caused by mutations in the VPS51 subunit of the GARP and EARP complexes. *Hum. Mol. Genet.* 28:1548–1560. https://doi.org/10.1093/hmg/ddy423

Gillingham, A.K., R. Sinka, I.L. Torres, K.S. Lilley, and S. Munro. 2014. Toward a comprehensive map of the effectors of rab GTPases. *Dev. Cell.* 31:358–373. https://doi.org/10.1016/j.devcel.2014.10.007

Gotthardt, K., M. Lokaj, C. Koerner, N. Falk, A. Gießl, and A. Wittinghofer. 2015. A G-protein activation cascade from Arl13B to Arl3 and implications for ciliary targeting of lipidated proteins. *eLife.* 4:e11859. https://doi.org/10.7554/eLife.11859

Griffiths, G., and K. Simons. 1986. The trans Golgi network: Sorting at the exit site of the Golgi complex. *Science.* 234:438–443. https://doi.org/10.1126/science.2945253

Guo, Y., G. Zanetti, and R. Schekman. 2013. A novel GTP-binding protein-adaptor protein complex responsible for export of Vangl2 from the trans Golgi network. *eLife.* 2:e00160.

Guo, Y., D.W. Sirkis, and R. Schekman. 2014. Protein sorting at the trans-Golgi network. *Annu. Rev. Cell Dev. Biol.* 30:169–206. https://doi.org/10.1146/annurev-cellbio-100913-013012

Hady-Cohen, R., H. Ben-Pazi, V. Adir, K. Yosovich, L. Blumkin, T. Lerman-Sagie, and D. Lev. 2018. Progressive cerebello-cerebral atrophy and progressive encephalopathy with edema, hypsarrhythmia and optic atrophy may be allelic syndromes. *Eur. J. Paediatr. Neurol.* 22:1133–1138. https://doi.org/10.1016/j.ejpn.2018.07.003

Hierro, A., D.C. Gershlick, A.L. Rojas, and J.S. Bonifacino. 2015. Formation of tubulovesicular carriers from endosomes and their fusion to the trans-Golgi network. *Int. Rev. Cell Mol. Biol.* 318:159–202. https://doi.org/10.1016/bs.ircmb.2015.05.005

Houghton, F.J., P.L. Chew, S. Lodeho, B. Goud, and P.A. Gleeson. 2009. The localization of the Golgin GCC185 is independent of Rab6A/A' and Arl1. *Cell.* 138:787–794. https://doi.org/10.1016/j.cell.2009.05.048

Houghton, F.J., S.A. Bellingham, A.F. Hill, D. Bourges, D.K. Ang, T. Gemetzis, I. Gasnereau, and P.A. Gleeson. 2012. Arl5b is a Golgi-localised small G protein involved in the regulation of retrograde transport. *Exp. Cell Res.* 318:464–477. https://doi.org/10.1016/j.yexcr.2011.12.023

Ivanova, A.A., T. Caspary, N.T. Seyfried, D.M. Duong, A.B. West, Z. Liu, and R.A. Kahn. 2017. Biochemical characterization of purified mammalian ARL13B protein indicates that it is an atypical GTPase and ARL3 guanine nucleotide exchange factor (GEF). *J. Biol. Chem.* 292:11091–11108. https://doi.org/10.1074/jbc.M117.784025

Jochum, A., D. Jackson, H. Schwarz, R. Pipkorn, and B. Singer-Krüger. 2002. Yeast Ysl2p, homologous to Sec7 domain guanine nucleotide exchange factors, functions in endocytosis and maintenance of vacuole integrity and interacts with the Arf-Like small GTPase Arl1p. *Mol. Cell. Biol.* 22:4914–4928. https://doi.org/10.1128/MCB.22.13.4914-4928.2002

Johannes, L., and B. Goud. 1998. Surfing on a retrograde wave: How does Shiga toxin reach the endoplasmic reticulum? *Trends Cell Biol.* 8:158–162. https://doi.org/10.1016/S0962-8924(97)01209-9

Karlsson, P., A. Droce, J.M. Moser, S. Cuhlmann, C.O. Padilla, P. Heimann, J.W. Bartsch, A. Füchtbauer, E.M. Füchtbauer, and T. Schmitt-John. 2013. Loss of vps54 function leads to vesicle traffic impairment, protein mis-sorting and embryonic lethality. *Int. J. Mol. Sci.* 14:10908–10925. https://doi.org/10.3390/ijms140610908

Kulak, N.A., G. Pichler, I. Paron, N. Nagaraj, and M. Mann. 2014. Minimal, encapsulated proteomic-sample processing applied to copy-number estimation in eukaryotic cells. *Nat. Methods.* 11:319–324. https://doi.org/10.1038/nmeth.2834

Lieu, Z.Z., M.C. Derby, R.D. Teasdale, C. Hart, P. Gunn, and P.A. Gleeson. 2007. The golgin GCC88 is required for efficient retrograde transport of cargo from the early endosomes to the trans-Golgi network. *Mol. Biol. Cell.* 18:4979–4991. https://doi.org/10.1091/mbc.e07-06-0622

Liewen, H., I. Meinhold-Heerlein, V. Oliveira, R. Schwarzenbacher, G. Luo, A. Wadle, M. Jung, M. Pfreundschuh, and F. Stenner-Liewen. 2005. Characterization of the human GARP (Golgi associated retrograde protein) complex. *Exp. Cell Res.* 306:24–34. https://doi.org/10.1016/j.yexcr.2005.01.022

Lu, L., and W. Hong. 2003. Interaction of Arl1-GTP with GRIP domains recruits autoantigens Golgin-97 and Golgin-245/p230 onto the Golgi. *Mol. Biol. Cell.* 14:3767–3781. https://doi.org/10.1091/mbc.e03-01-0864

Lu, L., and W. Hong. 2014. From endosomes to the trans-Golgi network. *Semin. Cell Dev. Biol.* 31:30–39. https://doi.org/10.1016/j.semcdb.2014.04.024

Lu, L., G. Tai, and W. Hong. 2004. Autoantigen Golgin-97, an effector of Arl1 GTPase, participates in traffic from the endosome to the trans-golgi network. *Mol. Biol. Cell.* 15:4426–4443. https://doi.org/10.1091/mbc.e03-12-0872

Ma, T., B. Li, R. Wang, P.K. Lau, Y. Huang, L. Jiang, R. Schekman, and Y. Guo. 2018. A mechanism for differential sorting of the planar cell polarity proteins Frizzled6 and Vangl2 at the trans-Golgi network. *J. Biol. Chem.* 293:8410–8427. https://doi.org/10.1074/jbc.RA118.001906

Mallard, F., B.L. Tang, T. Galli, D. Tenza, A. Saint-Pol, X. Yue, C. Antony, W. Hong, B. Goud, and L. Johannes. 2002. Early/recycling endosomes-to-TGN transport involves two SNARE complexes and a Rab6 isoform. *J. Cell Biol.* 156:653–664. https://doi.org/10.1083/jcb.200110081

Matsui, T., T. Itoh, and M. Fukuda. 2011. Small GTPase Rab12 regulates constitutive degradation of transferrin receptor. *Traffic.* 12:1432–1443. https://doi.org/10.1111/j.1600-0854.2011.01240.x

Nishimoto-Morita, K., H.W. Shin, H. Mitsuhashi, M. Kitamura, Q. Zhang, L. Johannes, and K. Nakayama. 2009. Differential effects of depletion of ARL1 and ARFRP1 on membrane trafficking between the trans-Golgi network and endosomes. *J. Biol. Chem.* 284:10583–10592. https://doi.org/10.1074/jbc.M900847200

Ortiz, D., M. Medkova, C. Walch-Solimena, and P. Novick. 2002. Ypt32 recruits the Sec4p guanine nucleotide exchange factor, Sec2p, to secretory vesicles; evidence for a Rab cascade in yeast. *J. Cell Biol.* 157:1005–1015. https://doi.org/10.1083/jcb.200201003

Panic, B., O. Perisic, D.B. Veprintsev, R.L. Williams, and S. Munro. 2003a. Structural basis for Arl1-dependent targeting of homodimeric GRIP domains to the Golgi apparatus. *Mol. Cell.* 12:863–874. https://doi.org/10.1016/S1097-2765(03)00356-3

Panic, B., J.R. Whyte, and S. Munro. 2003b. The ARF-like GTPases Arl1p and Arl3p act in a pathway that interacts with vesicle-tethering factors at the Golgi apparatus. *Curr. Biol.* 13:405–410. https://doi.org/10.1016/S0960-9822(03)00091-5

Pérez-Victoria, F.J., and J.S. Bonifacino. 2009. Dual roles of the mammalian GARP complex in tethering and SNARE complex assembly at the trans-Golgi network. *Mol. Cell. Biol.* 29:5251–5263. https://doi.org/10.1128/MCB.00495-09

Pérez-Victoria, F.J., G.A. Mardones, and J.S. Bonifacino. 2008. Requirement of the human GARP complex for mannose 6-phosphate-receptor-dependent sorting of cathepsin D to lysosomes. *Mol. Biol. Cell.* 19:2350–2362. https://doi.org/10.1091/mbc.e07-11-1189

Pérez-Victoria, F.J., G. Abascal-Palacios, I. Tascón, A. Kajava, J.G. Magadán, E.P. Pioro, J.S. Bonifacino, and A. Hierro. 2010a. Structural basis for the wobbler mouse neurodegenerative disorder caused by mutation in the Vps54 subunit of the GARP complex. *Proc. Natl. Acad. Sci. USA.* 107:12860–12865. https://doi.org/10.1073/pnas.1004756107

Pérez-Victoria, F.J., C. Schindler, J.G. Magadán, G.A. Mardones, C. Delevoye, M. Romao, G. Raposo, and J.S. Bonifacino. 2010b. Ang2/fat-free is a conserved subunit of the Golgi-associated retrograde protein complex. *Mol. Biol. Cell.* 21:3386–3395. https://doi.org/10.1091/mbc.e10-05-0392

Pfeffer, S.R. 2017. Rab GTPases: Master regulators that establish the secretory and endocytic pathways. *Mol. Biol. Cell.* 28:712–715. https://doi.org/10.1091/mbc.e16-10-0737

Pusapati, G.V., G. Luchetti, and S.R. Pfeffer. 2012. Ric1-Rgp1 complex is a guanine nucleotide exchange factor for the late Golgi Rab6A GTPase and an effector of the medial Golgi Rab33B GTPase. *J. Biol. Chem.* 287:42129–42137. https://doi.org/10.1074/jbc.M112.414565

Quenneville, N.R., T.Y. Chao, J.M. McCaffery, and E. Conibear. 2006. Domains within the GARP subunit Vps54 confer separate functions in complex assembly and early endosome recognition. *Mol. Biol. Cell.* 17:1859–1870. https://doi.org/10.1091/mbc.e05-11-1002

Reddy, J.V., A.S. Burguete, K. Sridevi, I.G. Ganley, R.M. Nottingham, and S.R. Pfeffer. 2006. A functional role for the GCC185 golgin in mannose 6-phosphate receptor recycling. *Mol. Biol. Cell.* 17:4353–4363. https://doi.org/10.1091/mbc.e06-02-0153

Rosa-Ferreira, C., C. Christis, I.L. Torres, and S. Munro. 2015. The small G protein Arl5 contributes to endosome-to-Golgi traffic by aiding the recruitment of the GARP complex to the Golgi. *Biol. Open.* 4:474–481. https://doi.org/10.1242/bio.201410975

Schindler, C., Y. Chen, I. Pu, X. Guo, and J.S. Bonifacino. 2015. EARP is a multisubunit tethering complex involved in endocytic recycling. *Nat. Cell Biol.* 17:639–650. https://doi.org/10.1038/ncb3129

Schmitt-John, T., C. Drepper, A. Mussmann, P. Hahn, M. Kuhlmann, C. Thiel, M. Hafner, A. Lengeling, P. Heimann, J.M. Jones, et al. 2005. Mutation of Vps54 causes motor neuron disease and defective spermiogenesis in the wobbler mouse. *Nat. Genet.* 37:1213–1215. https://doi.org/10.1038/ng1661

Schürmann, A., S. Massmann, and H.G. Joost. 1995. ARP is a plasma membrane-associated Ras-related GTPase with remote similarity to the family of ADP-ribosylation factors. *J. Biol. Chem.* 270:30657–30663. https://doi.org/10.1074/jbc.270.51.30657

Setty, S.R., M.E. Shin, A. Yoshino, M.S. Marks, and C.G. Burd. 2003. Golgi recruitment of GRIP domain proteins by Arf-like GTPase 1 is regulated by Arf-like GTPase 3. *Curr. Biol.* 13:401–404. https://doi.org/10.1016/S0960-9822(03)00089-7

Setty, S.R., T.I. Strochlic, A.H. Tong, C. Boone, and C.G. Burd. 2004. Golgi targeting of ARF-like GTPase Arl3p requires its Nα-acetylation and the integral membrane protein Sys1p. *Nat. Cell Biol.* 6:414–419. https://doi.org/10.1038/ncb1121

Shin, H.W., H. Kobayashi, M. Kitamura, S. Waguri, T. Suganuma, Y. Uchiyama, and K. Nakayama. 2005. Roles of ARFRP1 (ADP-ribosylation factor-related protein 1) in post-Golgi membrane trafficking. *J. Cell Sci.* 118:4039–4048. https://doi.org/10.1242/jcs.02524

Siniossoglou, S., and H.R. Pelham. 2001. An effector of Ypt6p binds the SNARE Tlg1p and mediates selective fusion of vesicles with late Golgi membranes. *EMBO J.* 20:5991–5998. https://doi.org/10.1093/emboj/20.21.5991

Siniossoglou, S., and H.R. Pelham. 2002. Vps51p links the VFT complex to the SNARE Tlg1p. *J. Biol. Chem.* 277:48318–48324. https://doi.org/10.1074/jbc.M209428200

Sugimoto, M., M. Kondo, M. Hirose, M. Suzuki, K. Mekada, T. Abe, H. Kiyonari, A. Ogura, N. Takagi, K. Artzt, et al. 2012. Molecular identification of t(w5): Vps52 promotes pluripotential cell differentiation through cell-cell interactions. *Cell Reports.* 2:1363–1374. https://doi.org/10.1016/j.celrep.2012.10.004

Sztul, E., P.W. Chen, J.E. Casanova, J. Cherfils, J.B. Dacks, D.G. Lambright, F.S. Lee, P.A. Randazzo, L.C. Santy, A. Schürmann, et al. 2019. ARF GTPases and their GEFs and GAPs: Concepts and challenges. *Mol. Biol. Cell.* 30:1249–1271. https://doi.org/10.1091/mbc.E18-12-0820

Torres, I.L., C. Rosa-Ferreira, and S. Munro. 2014. The Arf family G protein Arl1 is required for secretory granule biogenesis in *Drosophila*. *J. Cell Sci.* 127:2151–2160. https://doi.org/10.1242/jcs.122028

Uwineza, A., J.H. Caberg, J. Hitayezu, S. Wenric, L. Mutesa, Y. Vial, S. Drunat, S. Passemard, A. Verloes, V. El Ghouzzi, et al. 2019. VPS51 biallelic variants cause microcephaly with brain malformations: A confirmatory report. *Eur. J. Med. Genet.* 62:103704. https://doi.org/10.1016/j.ejmg.2019.103704

Wakade, R., H. Labbaoui, D. Stalder, R.A. Arkowitz, and M. Bassilana. 2017. Overexpression of YPT6 restores invasive filamentous growth and secretory vesicle clustering in a Candida albicans arl1 mutant. *Small GTPases.* 29:1–7. https://doi.org/10.1080/21541248.2017.1378157

Wong, M., and S. Munro. 2014. The specificity of vesicle traffic to the Golgi is encoded in the golgin coiled-coil proteins. *Science.* 346:1256898. https://doi.org/10.1126/science.1256898

Wu, M., L. Lu, W. Hong, and H. Song. 2004. Structural basis for recruitment of GRIP domain golgin-245 by small GTPase Arl1. *Nat. Struct. Mol. Biol.* 11:86–94. https://doi.org/10.1038/nsmb714

Yoshino, A., S.R. Setty, C. Poynton, E.L. Whiteman, A. Saint-Pol, C.G. Burd, L. Johannes, E.L. Holzbaur, M. Koval, J.M. McCaffery, et al. 2005. tGolgin-1 (p230, golgin-245) modulates Shiga-toxin transport to the Golgi and Golgi motility towards the microtubule-organizing centre. *J. Cell Sci.* 118:2279–2293. https://doi.org/10.1242/jcs.02358

Yu, I.M., and F.M. Hughson. 2010. Tethering factors as organizers of intracellular vesicular traffic. *Annu. Rev. Cell Dev. Biol.* 26:137–156. https://doi.org/10.1146/annurev.cellbio.042308.113327

Zahn, C., A. Hommel, L. Lu, W. Hong, D.J. Walther, S. Florian, H.G. Joost, and A. Schürmann. 2006. Knockout of Arfrp1 leads to disruption of ARF-like1 (ARL1) targeting to the trans-Golgi in mouse embryos and HeLa cells. *Mol. Membr. Biol.* 23:475–485. https://doi.org/10.1080/09687860600840100

Zahn, C., A. Jaschke, J. Weiske, A. Hommel, D. Hesse, R. Augustin, L. Lu, W. Hong, S. Florian, A. Scheepers, et al. 2008. ADP-ribosylation factor-like GTPase ARFRP1 is required for trans-Golgi to plasma membrane trafficking of E-cadherin. *J. Biol. Chem.* 283:27179–27188. https://doi.org/10.1074/jbc.M802108200